

# Mitigation of Anomalous Ionosphere Threat to Enhance Utility of LAAS Differentially Corrected Positioning Service (DCPS)

Young Shin Park, Sam Pullen, and Per Enge

Stanford University

496 Lomita Mall

Stanford, CA 94305 USA

**Abstract-**Local Area Augmentation System (LAAS) can be used for both Category I (CAT I) precision approach and Differentially Corrected Positioning Service (DCPS) navigation applications. Through its support of DCPS, the LAAS Ground Facility (LGF) is required to help meet the integrity requirements of terminal-area navigation and other operations that could use the LAAS VHF Data Broadcast in addition to precision approach. The current LAAS standards indicate that DCPS integrity risk shall not exceed  $10^{-7}$  per hour [1,2]. This paper demonstrates that the requirement in current LAAS standards is hard to achieve under anomalous ionosphere and proposes potential requirements changes to improve DCPS availability. Horizontal Position Error (HPE) is calculated from current ionosphere threat model and is applied to individual satellites in all the subset geometries. Limited subset geometries and screening Horizontal Alert Limit (HAL) are considered as requirements changes of current LAAS MOPS for DCPS. Limited subset geometries with drill down to N-2 satellites (or SV's) mitigate maximum unbounded HPE caused from 6 kilometers to 110 meters. The screening HAL of 550 meters allows maximum HPE of 300 meters.

## I. INTRODUCTION

### A. Local Area Augmentation System (LAAS)

The Local Area Augmentation System (LAAS) shown in Fig. 1 is a ground-based augmentation to GPS that focuses its service on the airport area, approximately a 20-30 mile radius, for precision approach, terminal area operations and airport surface movement. LAAS is comprised of ground facility and avionics. The LAAS Ground Facility (LGF) includes 4 reference receivers, LAAS ground processors, and a VHF data broadcast (VDB) transmitter. This ground facility is complemented by LAAS avionics installed on the aircraft. Signals from GPS satellites are received by the LAAS GPS reference receivers at the LAAS-equipped airport. The reference receivers calculate their position using GPS. The GPS reference receivers and LAAS Ground Processors work together to measure errors in GPS-provided position. The LAAS ground processors produce a LAAS correction

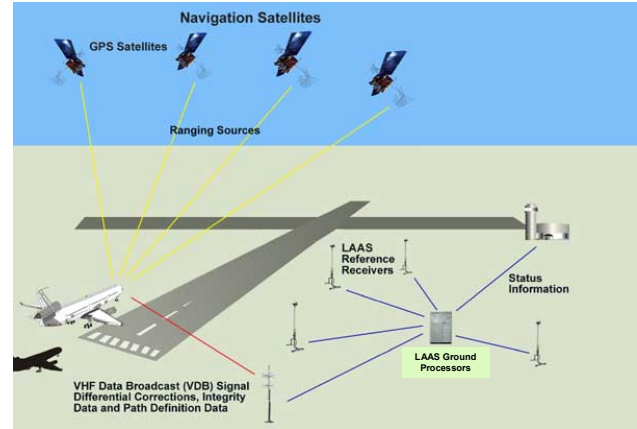


Fig. 1. Local Area Augmentation System (LAAS) [1].

message based on the difference between actual and GPS-calculated position. Included in this message is suitable integrity parameters and approach path information. This LAAS correction message is then sent to a VDB transmitter. The VDB broadcasts the LAAS signal throughout the LAAS coverage area to avionics in LAAS-equipped aircraft. The signal coverage is designed to support the aircraft's transition from en route airspace into and throughout the terminal area airspace. The LAAS equipment in the aircraft uses the corrections provided on position, velocity, and time to guide the aircraft safely to the runway. This signal provides ILS-look-alike guidance as low as 200 feet above touchdown. LAAS will eventually support landings all the way to the runway surface [3].

The primary service that LAAS provides is precision approach and the secondary service is terminal area operations, aircraft operations in terminal area airspace, and airport surface movement, aircraft movement on the ground of airport such as taxiing. Differentially Corrected Positioning Service (DCPS) is an extension of LAAS capability to support terminal area operations and airport surface movement. Through its support of DCPS, the LAAS Ground Facility (LGF) is required to help meet the integrity requirements of terminal-area navigation and

other operations that could use the LAAS VHF Data Broadcast in addition to precision approach. The current LAAS standards indicate that DCPS integrity risk shall not exceed  $10^{-7}$  per hour [1,2]. This requirement is hard to achieve under the severe error sources such as anomalous ionosphere which has been observed over CONUS since 2000 [4,5].

#### B. Ionosphere Anomaly Threat Model

One of the residual errors that can be built up for the user of a dGPS system like LAAS is the ionosphere spatial decorrelation error. This error is caused by the fact that two signals are passing through different region of the atmosphere and the ionospheric delays cannot be completely canceled out even after applying differential corrections. Such errors can grow under severe ionosphere storm and pose a threat to user integrity [6].

The ionosphere, extending from a height of about 50 kilometers to about 1000 kilometers above the earth, is a region of ionized gases (from electrons and ions). The ionization is caused by the sun's radiation, and the state of the ionosphere is determined primarily by the intensity of the solar activity. Solar flares and the resulting magnetic storms can create large and quickly varying electron densities, causing rapid fluctuation in the carrier phase (called scintillation) and in amplitude (called fading) of GPS signals [7].

As described in our previous work (see [8,9,10]), ionosphere anomalies are modeled as linear wave fronts in order to study their impact on a LAAS user. Fig. 2 illustrates this simplified model and an example of the ionosphere anomaly threat to LAAS. Four parameters are used to characterize the anomaly: gradient slope (in millimeters per kilometer), gradient width (in kilometers), front speed (in meters per second), and maximum delay difference (in meters), which is simply the product of gradient slope and width. Upper bounds on each of these parameters have been determined based on analysis of past storms. Note that the maximum delay difference is also expressed as an upper bound in the model, and it constrains the slope and width values through their product (i.e., values of slope and width which are within

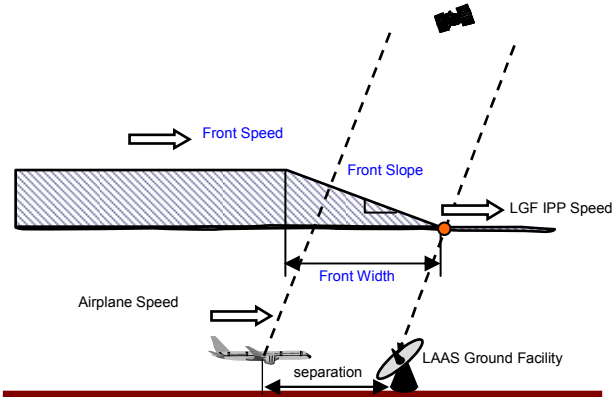


Fig. 2. Ionosphere wave front model.

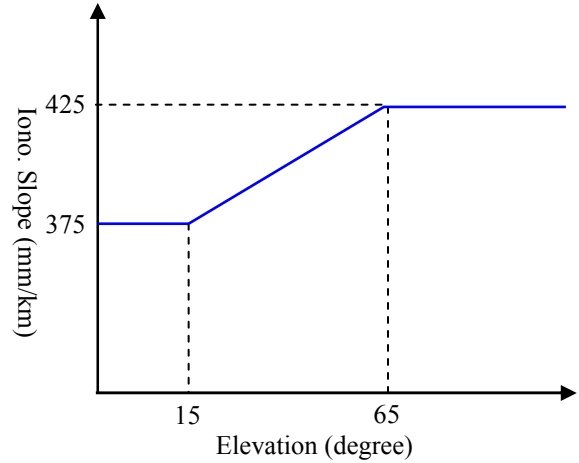


Fig. 3. Ionosphere anomaly threat model  
(Slope Bounds Last Updated in March 2007).

their respective bounds but exceed the maximum-delay-difference bound when multiplied together are not a valid combination) [4,5].

As noted above, the parameters in the simplified model of ionosphere anomaly are estimated using data collected on ionosphere stormy days, and they can be summarized by an ionosphere anomaly “threat model.” The current ionosphere anomaly threat model (most recently revised in March 2007) is as shown in Fig. 3, in which the slant ionosphere gradient is 375 millimeters per kilometer for low elevation of satellite below 15 degrees and 425 millimeters per kilometer for high elevation above 65 degrees. In between, slant ionosphere gradient is a linear function of the elevation angle of satellite (the bounds on speed, width, and maximum delay difference remain the same as the numbers given in [11]). The threat model is used to generate range error caused by anomalous ionosphere.

#### C. Precision Approach and DCPS

In our previous work, LGF real time geometry screening has been developed to mitigate ionosphere anomaly threat for LAAS CAT I precision approach. The algorithm in [11] inflates the sigma values ( $\sigma_{\text{vig}}$  and  $\sigma_{\text{pr_gn}}$ ) broadcast by the LGF. This ensures that subset satellite geometries (i.e. subsets of a set of approved GPS satellites for which the LGF broadcasts valid corrections) for which unacceptable errors can result are made unavailable to the user. These unsafe subsets are found by comparing the resulting Maximum Ionosphere-induced Error in Vertical (MIEV) with maximum “safe” Navigation System Error (NSE) values derived from Obstacle Clearance Surface (OCS) applicable to CAT I precision approaches. Another algorithm in [12] implements LGF real time geometry screening by inflating satellite-specific, targeted ephemeris decorrelation parameters (called “P-values”) and  $\sigma_{\text{pr_gn}}$  values. These algorithms are briefly illustrated in the flow chart in Fig. 4. From satellites almanac,

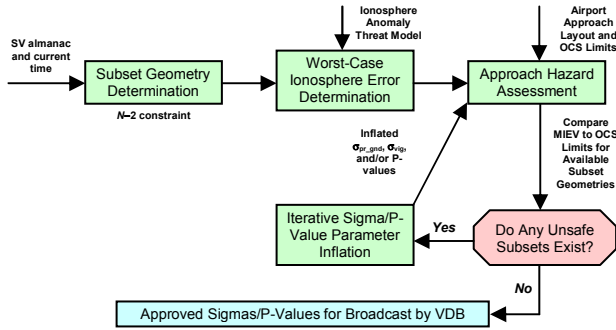


Fig. 4. Ionosphere anomaly mitigation for LAAS CAT I precision approach.

subset geometries are determined and worst-case ionosphere error is determined from ionosphere anomaly threat model. Then, approach hazard assessment is applied and if unsafe subsets exist, it inflates sigma and P-value parameter iteratively to make all subsets safe. Finally, approved sigma values and P-values for broadcast by VDB are obtained. Our previous papers demonstrate that geometry screening in LAAS can fully mitigate the CONUS ionosphere spatial decorrelation threat model [11, 12].

This method works reasonably well for precision approach applications, where the Vertical Alert Limit (VAL) and OCS limits for precision approaches are well-defined, but it cannot be directly transported to the DCPS application because no single Horizontal Alert Limit (HAL) is defined for DCPS. This is because DCPS is intended to support a variety of terminal area operations with different values of HAL; thus no one HAL can be used to define DCPS integrity. The comparison between precision approach and DCPS is summarized in Table I. Precision approach has known operation and known VAL, and may also have constrained subset geometries. Therefore, LGF knows what geometries are hazardous and can take an action to get rid of them. DCPS has many different operations and their HAL values are not defined. Therefore, LGF cannot take any action to take care of hazardous geometries. For this reason, the existing LAAS requirements call for Horizontal Protection Level (HPL) to always exceed the maximum HPE, but the results in [6] show that this is not possible in the face of the ionosphere

TABLE I  
COMPARISON BETWEEN PRECISION APPROACH AND DCPS

Precision Approach	DCPS
Known operation	Many different operations
Known VAL	Undefined HAL values
Constrained subset geometries	No constraints on subset geometries
Action to get rid of hazardous geometries	No action to take care of hazardous geometries

anomalies observed in October and November of 2003 unless the resulting HPL is inflated to be hundreds or thousands of meters.

Given that the existing DCPS integrity requirements cannot be met in the presence of the very worst ionosphere anomalies observed in the past, this paper examines several possible system modifications to make DCPS more useful. One approach examined requires changes to the LAAS MOPS [13] – constraints are imposed on airborne geometry screening. The second approach investigated is to mandate screening HAL value taken for all the terminal-area operations from RTCA DO-236B [14]. This paper considers the various modifications taken together and recommends a way forward to enhance the availability and utility of DCPS without significantly affecting the safety of DCPS users.

## II. DCPS SIMULATION PROCEDURE

DCPS simulation procedure is shown in Fig. 5. One day of geometries with five minutes updates from Memphis airport is used to generate all in view, all N-1, all N-2, ..., down to all 4 satellites subset geometries. Range error from ionosphere threat model is applied to all independent individual satellites in those subset geometries.  $\sigma_{\text{sig}}$  of 18.4 millimeters per kilometer which is based on approximate maximum LGF inflation factor of 4.6 is used. Then computed HPE and HPL are obtained, and only worst HPE and corresponding HPL are saved. When we consider possible requirements changes, geometry screening with screening HAL is applied so that only points whose HPL values are less than screening HAL are survived. Finally maximum HPE with specific screening HAL is obtained.

DCPS simulation is applied to three scenarios specified in Table II. 5-km LGF-to-user separation represents airport surface, and the altitude of zero meter and the aircraft speed of zero meter per second are used for the first scenario. 15-km LGF-to-user separation represents terminal area inside LAAS coverage, and 45-km LGF-to-user separation represents at the edge of LAAS coverage,

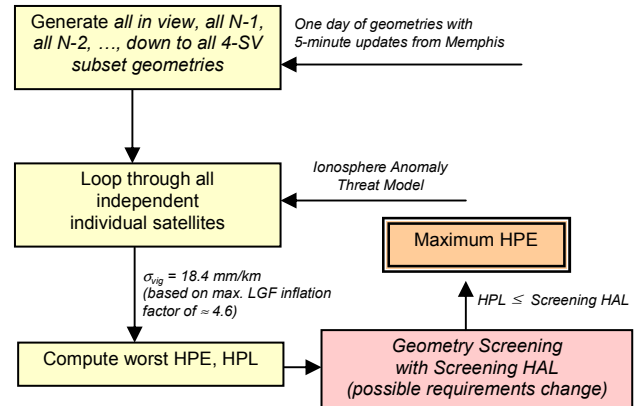


Fig. 5. DCPS simulation procedure.

TABLE II  
DCPS SCENARIO

Scenario No.	Description	x (km)	Altitude (m)*
1	Airport Surface	5	0
2	Terminal Area, Inside LAAS Coverage	15	3000
3	At Edge of LAAS Coverage ( $D_{max}$ )	45	3000

\*Altitude makes little difference to DCPS error results.

which is VDB coverage. The second and third scenarios use altitude of 3000 meters and aircraft speed of 70 meters per second.

### III. IONOSPHERE ANOMALY IMPACT ON 1 SV

#### A. Effect of Geometry on HPE

Fig. 6 shows HPE versus HPE-to-HPL ratio plot of ionosphere anomaly impact on 1 satellite with drill down to 4-SV geometries for 45-km LGF-to-user separation case. The point in magenta circle indicates its maximum HPE which is approximately 267 kilometers. This large error is caused by its bad geometry which is shown in Fig. 7. Its geometry has only four satellites which is the smallest number of satellites allowed in the geometry for DCPS. The  $S_{\text{horizontal}}$  values of four satellites in Fig. 7 are shown in Table III. Here, the S matrix is the inverse matrix of the G matrix and it produces position error by being multiplied by range errors of satellites in geometry.  $S_{\text{horizontal}}$  value is horizontal component of the S matrix. The  $S_{\text{horizontal}}$  values in Table III are big enough to produce this large HPE. Shaded satellite in Fig. 7 and Table III indicates one impacted by ionosphere anomaly. The worst HPE is calculated when satellite No. 3 is chosen to be impacted in this geometry because  $S_{\text{horizontal}}$  value of this satellite is the biggest. The corresponding all-in-view geometry to the maximum HPE and its  $S_{\text{horizontal}}$  values are shown in Fig. 8 and Table IV, respectively. It has three more satellites in green oval at high elevation, total seven satellites and they are distributed well in elevation and azimuth. Impact on satellite No. 6 produces the worst HPE in this all-in-view geometry because its elevation is so high, above 65 degrees, that its range error calculated from ionosphere anomaly threat model is the biggest. Although its  $S_{\text{horizontal}}$  value is the lowest among satellites in the geometry, differences of range errors among satellites are bigger than differences of  $S_{\text{horizontal}}$  values, so that effect of the range error is bigger than the effect of the  $S_{\text{horizontal}}$  value. The HPE corresponding to this all-in-view geometry is approximately 10 meters which is a point in green circle in Fig. 6 and it is the smallest among all the subset geometries of this all-in-view geometry.

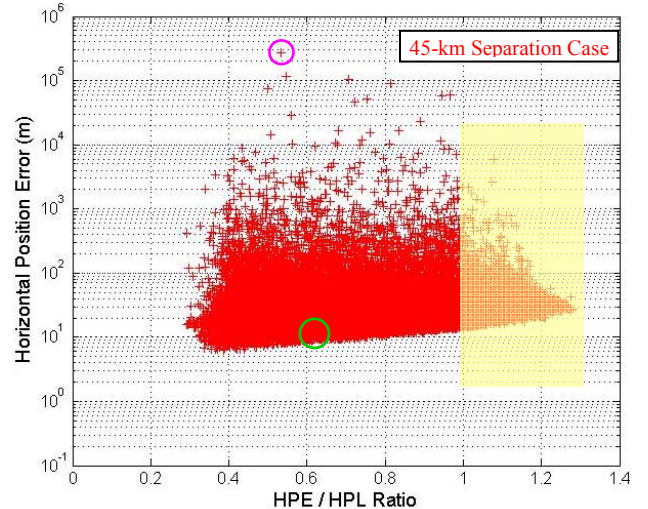


Fig. 6. HPE versus HPE-to-HPL ratio plot of ionosphere anomaly impact on 1 SV with drill down to 4 SV's for 45-km separation case.

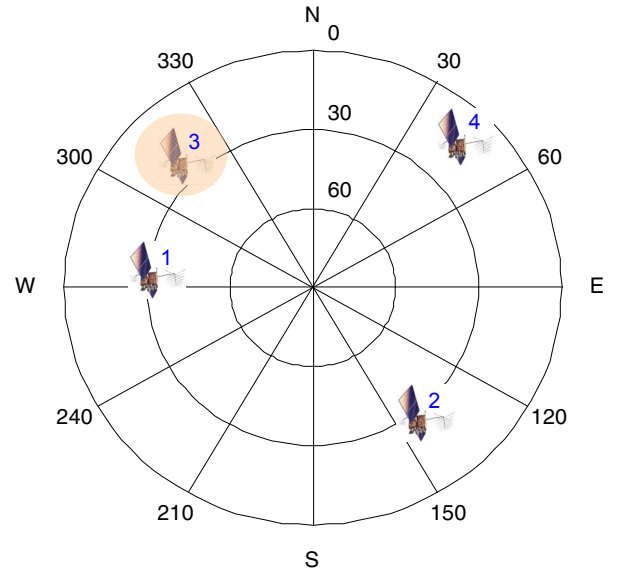


Fig. 7. Sky plot of corresponding geometry to maximum HPE of ionosphere anomaly impact on 1 SV with drill down to 4 SV's for 45-km separation case.

TABLE III  
 $S_{\text{horizontal}}$  VALUES OF SATELLITES IN FIG. 7

SV No.	$S_{\text{horizontal}}$
1	13548
2	5525
3	15496
4	7473

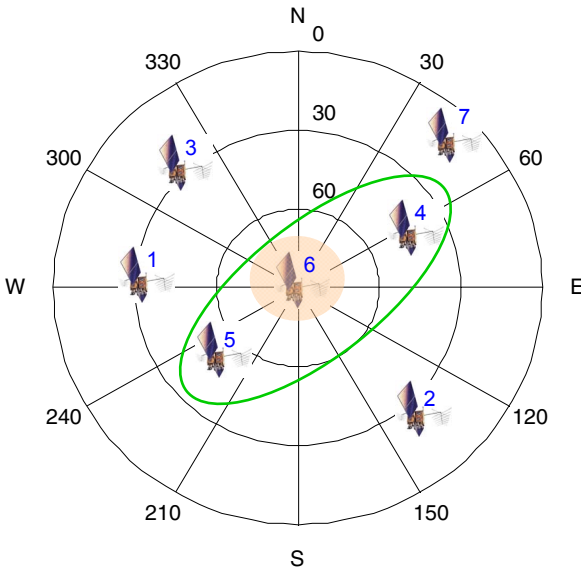


Fig. 8. Sky plot of all-in-view geometry corresponding to the maximum HPE of ionosphere anomaly impact on 1 SV with drill down to 4 SV's for 45-km separation case.

TABLE IV  
 $S_{\text{horizontal}}$  VALUES OF SATELLITES IN FIG. 8

SV No.	$S_{\text{horizontal}}$
1	0.3446
2	0.6415
3	0.3812
4	0.3733
5	0.3463
6	0.1625
7	0.3633

### B. Effect of Separation on DCPS

HPE versus HPE-to-HPL plots of the ionosphere anomaly impact on 1 SV with dill down to 4 satellites for the 15-km LGF-to-user separation case and for the 5-km LGF-to-user separation case are shown in blue in Fig. 9 and in green in Fig. 10, respectively. Red points in Fig. 9 and Fig. 10 represent the 45-km LGF-to-user separation case, the same as in Fig. 6. The maximum HPE is approximately 90 kilometers for the 15-km LGF-to-user separation case and 30 kilometers for the 5-km LGF-to-user separation case. These two separation cases does not have any points whose HPE-to-HPL ratios exceed 1, which means their HPE values are always less than their HPL values, while the 45-km LGF-to-user separation case has some cases, shown in shaded region, whose HPE-to-HPL ratios exceed 1. In other words, the points in blue and green are protected by their HPL values, whereas some points in red are not protected by their HPL values. The maximum unbounded HPE for the 45-km LGF-to-user separation case is approximately 6 kilometers which is more hazardous than its maximum HPE of 267 kilometers since it is not bounded by its HPL. From the 15-km LGF-to-user separation case to the 45-km LGF-to-

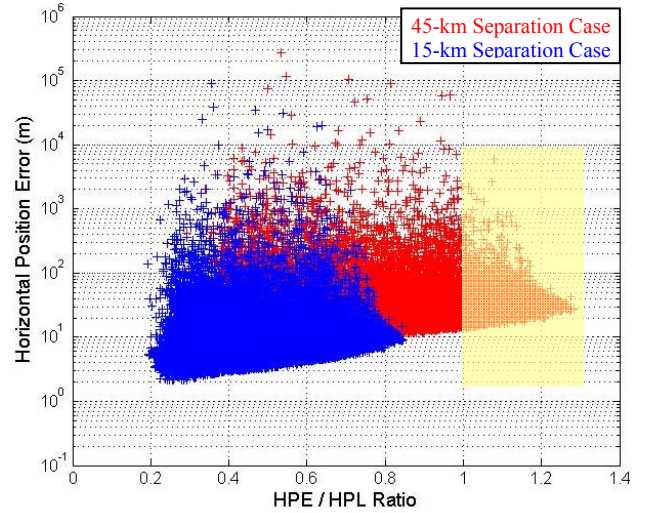


Fig. 9. HPE versus HPE-to-HPL ratio plot of ionosphere anomaly impact on 1 SV with drill down to 4 SV's for 45-km (red) and 15-km separation case (blue).

user separation case, it is monotonic increase of HPE-to-HPL ratio toward its value of 1. Approximately 21.5-km LGF-to-user separation case starts to have a point in the shaded region. The reason why the 5-km LGF-to-user separation case is not a component of monotonic increase is because different parameters are used for this case. The aircraft speed of zero meters per second and the altitude of zero meter are used for 5-km LGF-to-user separation case, while aircraft speed of 70 meters per seconds and altitude of 3000 meters are used for other separations.

5-km and 15-km LGF-to-user separation cases do not harm DCPS users, whereas some cases in 45-km LGF-to-user separation case do. The red points in shaded region are subjects to mitigate by changing requirements in current LAAS MOPS for DCPS.

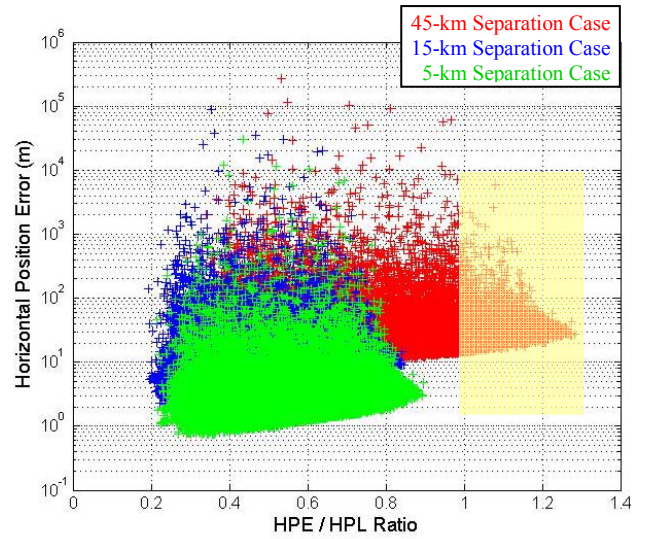


Fig. 10. HPE versus HPE-to-HPL ratio plot of ionosphere anomaly impact on 1 SV with drill down to 4 SV's for 45-km (red), 15-km (blue), and 5-km separation case (green).

## IV. CHANGES TO IMPROVE DCPS AVAILABILITY

### A. Potential Requirements Changes

Three potential requirements changes to existing LAAS MOPS for DCPS are being considered. First change considered in this paper is limited subset geometries. It restricts DCPS users to specific subsets that can be protected. The current MOPS for DCPS allows all geometries with four or more satellites. Limited subset geometries allow, for example, all zero, one and two-satellite-out combinations which is called drill down to N-2 satellites. The second change considered is applying the screening HAL which specifies a uniform maximum HPL for all DCPS users. Since any HAL values are not defined in the current LAAS MOPS for DCPS, all DCPS users can determine their own HAL values according to their operations, e.g. 25 meters for airport surface movement. The screening HAL can provide a bound to DCPS users when they choose their own HAL values for their own operations. Supported operations with smaller HAL values would not be affected. The third change to be considered is airborne Code-Carrier Divergence (CCD) monitoring which will also be required for CAT-three precision approaches. The third change will be considered in the future work.

### B. Limited Subset Geometries

Effect of various limited subset geometries on HPE is examined for the ionosphere anomaly impact on 1 SV and 45-km LGF-to-user separation case. HPE versus HPE-to-HPL ratio plots with drill down to N-3 satellites, drill down to N-2 satellites, and drill down to N-1 satellites are shown in magenta in Fig. 11, in blue in Fig. 12, and in green in Fig. 13, respectively. The plot with drill down to 4 satellites is shown in red and it is the same as the plot in Fig. 6. The maximum unbounded HPE, the largest HPE whose ratio exceeds 1, for drill down to 4 satellites is approximately 6 kilometers. The maximum unbounded HPE with drill down to N-3 satellites is 6 kilometers, the same as one with drill down to 4 satellites, as well. Limited subset geometries with drill down to N-3 satellites do not mitigate the maximum unbounded HPE. The maximum unbounded HPE with drill down to N-2 satellites is approximately 110 meters which is much smaller than 6 kilometers and acceptable for terminal area operations. The maximum unbounded HPE with drill down to N-1 satellites is approximately 70 meters, the smallest among four limited subset geometries proposed. However, limited subset geometries with drill down to N-1 satellites are not realistic when aircraft maneuvering in terminal area airspace which includes banking is considered. Therefore, drill down to N-2 satellites is considered as proper limited subset geometries for DCPS to mitigate the maximum unbounded HPE which is a threat to DCPS users.

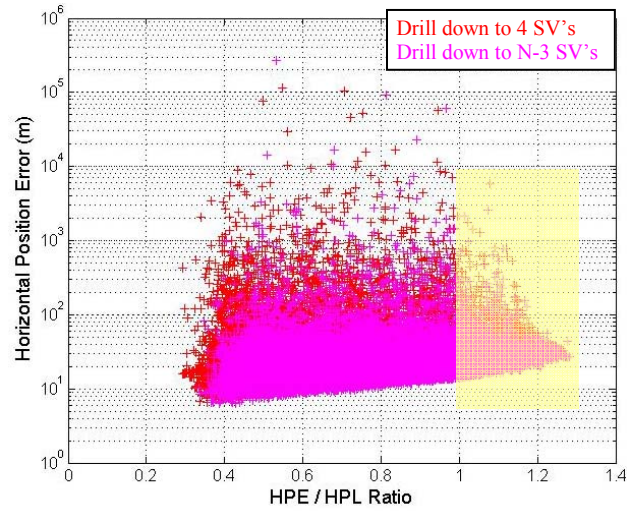


Fig. 11. HPE versus HPE-to-HPL ratio plot of ionosphere anomaly impact on 1 SV with drill down to 4 SV's (red), and drill down to N-3 SV's (magenta) for 45-km separation case.

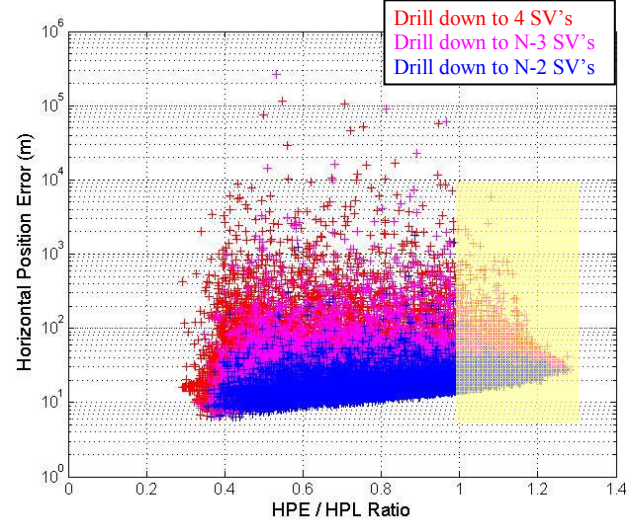


Fig. 12. HPE versus HPE-to-HPL ratio plot of ionosphere anomaly impact on 1 SV with drill down to 4 SV's (red), drill down to N-3 SV's (magenta), and drill down to N-2 SV's (blue) for 45-km separation case.

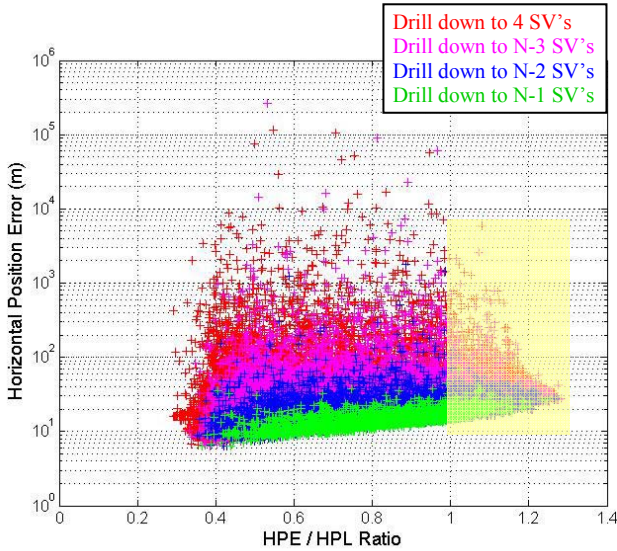


Fig. 13. HPE versus HPE-to-HPL ratio plot of ionosphere anomaly impact on 1 SV with drill down to 4 SV's (red), drill down to N-3 SV's (magenta), drill down to N-2 SV's (blue), and drill down to N-1 SV's (green) for 45-km separation case.

### C. Screening HAL

Fig. 14 and Fig. 15 shows HPE versus HPL plot of the ionosphere anomaly impact on 1 SV with drill down to 4 satellites and drill down to N-2 satellites for the 45-km LGF-to-user separation case, respectively. Drill down to 4 satellites is shown in red. If maximum HPE we allow is assumed to be 300 meters, the screening HAL should be 250 meters. Drill down to N-2 satellites is shown in blue, and the screening HAL should be 550 meters to allow the same 300 meters of maximum HPE. Here, it is confirmed that drill down to N-2 satellites allows DCPS users more flexible screening HAL values.

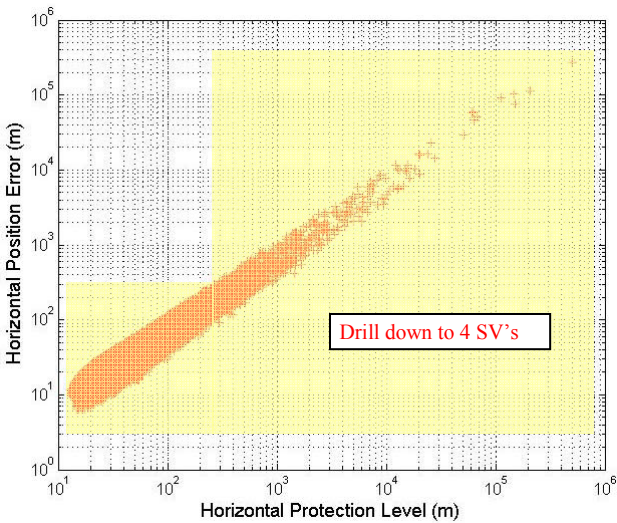


Fig. 14. HPE versus HPL plot of ionosphere anomaly impact on 1 SV with drill down to 4 SV's for 45-km separation case.

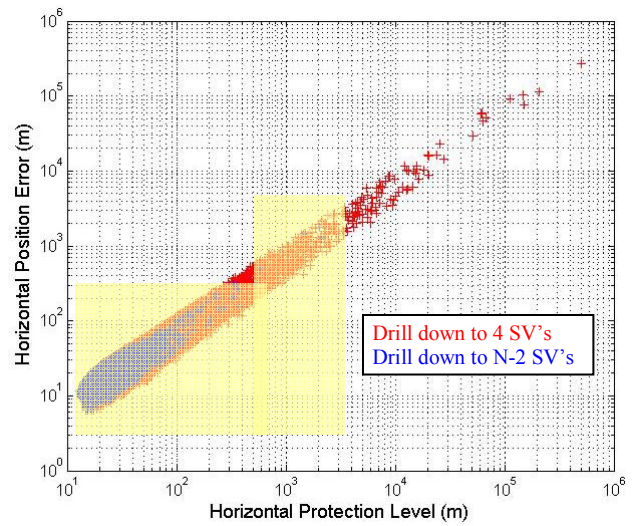


Fig. 15. HPE versus HPL plot of ionosphere anomaly impact on 1 SV with drill down to 4 SV's (red), and drill down to N-2 SV's (blue) for 45-km separation case.

## V. IONOSPHERE ANOMALY IMPACT ON 2 SV's

The preliminary result of ionosphere anomaly impact on 2 satellites with drill down to 4 satellites for the 5-km LGF-to-user separation case is shown in red in Fig. 16 and Fig. 17. The maximum unbound HPE in shaded area is approximately 10 kilometers. When it is compared to the result of impact on 1 SV for the same case of limited geometries and LGF-to-user separation in green in Fig. 17, it can be seen that ionosphere anomaly impact on one more satellite can cause to pose a threat to DCPS users by producing very larger position error. The ionosphere anomaly impact on 2 satellites is still investigated and is a subject of the future work.

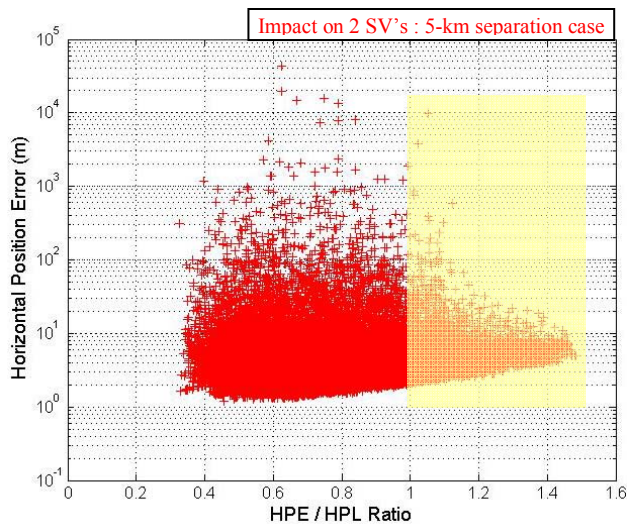


Fig. 16. HPE versus HPE-to-HPL ratio plot of ionosphere anomaly impact on 2 SV's with drill down to 4 SV's for 5-km separation case.

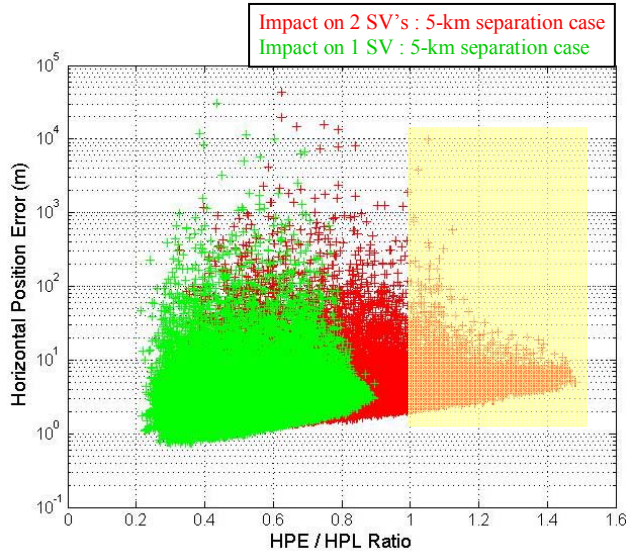


Fig. 17. HPE versus HPE-to-HPL ratio plot of ionosphere anomaly impact on 2 SV's (red) and 1 SV (green) with drill down to 4 SV's for 5-km separation case.

## VI. SUMMARY AND FUTURE WORK

DCPS will improve efficiency in terminal area operations and airport surface movement. This research shows DCPS integrity difficulty due to the ionosphere. For one satellite impact and 45-km LGF-to-user separation case, the maximum unbounded HPE is 6 kilometers, and for two satellites impact and 5-km LGF-to-user separation case, the maximum unbounded HPE is 10 kilometers. A solid way to solve difficulty explored in this paper for the ionosphere anomaly impact on one satellite includes N-2 restriction in geometries. It decreases maximum unbounded HPE from 6 kilometers to 110 meters. The way also includes the potential geometry screening using the screening HAL, for example, the screening HAL of 550 meters allows the maximum HPE of 300 meters for 45-km LGF-to-user separation case with the limited subset geometries of drill down to N-2 satellites.

Future work includes ionosphere anomaly impact on two satellites, more-flexible geometry restriction by limiting maximum  $S_{\text{horizontal}}$  at aircraft, and application of system changes i.e. airborne CCD monitoring.

## ACKNOWLEDGMENT

This research was supported by the Federal Aviation Administration (FAA) Local Area Augmentation System (LAAS) Program Office. Within the FAA, John Warburton and Jason Burns were particularly helpful. The opinions discussed here are those of the authors and do not necessarily represent those of the FAA or other affiliated agencies.

## REFERENCES

- [1] *Specification: Category I Local Area Augmentation System Ground Facility*. Washington, D.C., Federal Aviation Administration, FAA-E-2937A, April 17, 2002.
- [2] *Minimum Aviation System Performance Standards for the Local Area Augmentation System (LAAS)*. Washington, D.C., RTCA SC-159, WG-4A, DO-245A, December 9, 2004.
- [3] Federal Aviation Administration (FAA) – Navigation Services – Local Area Augmentation System (LAAS). URL: [http://www.faa.gov/about/office\\_org/headquarters\\_offices/ato/service\\_units/techops/navservices/gnss/laas/](http://www.faa.gov/about/office_org/headquarters_offices/ato/service_units/techops/navservices/gnss/laas/).
- [4] A. Ene, D. Qiu, M. Luo, S. Pullen, and P. Enge, “A Comprehensive Ionosphere Storm Data Analysis Method to Support LAAS Threat Model Development,” *Proceedings of ION 2005 National Technical Meeting*, San Diego, CA., January 15-20, 2005, pp. 110-130.
- [5] M. Luo, S. Pullen, s. Datta-Barua, G. Zhang, T. Walter, and P. Enge, “LAAS Study of Slow-Moving Ionosphere Anomalies and Their Potential Impacts,” *Proceedings of ION GNSS 2005*, Long Beach, CA, September 13-16, 2005, pp. 2337-2349.
- [6] Y. S. Park, G. Zhang, S. Pullen, J. Lee, and P. Enge, “Data-Replay Analysis of LAAS Safety during Ionosphere Storms,” *Proceedings of ION GNSS 2007*, Fort Worth, TX, September 25-28, 2007.
- [7] P. Misra, and P. Enge, *Global Positioning System: Signals, Measurements, and Performance*, 2<sup>nd</sup> ed., Gangam-Jamuna Press, Lincoln, MA, 2006, pp. 162-163.
- [8] M. Luo, S. Pullen, J. Dennis, H. Konno, G. Xie, T. Walter, S. Datta-Barua, T. Dehel, and Per Enge “LAAS Ionosphere Spatial Gradient Threat Model and Impact of LGF and Airborne Monitoring,” *Proceedings of ION GPS 2003*, Portland, OR., September 9-12, 2003, pp 2255-2274.
- [9] M. Luo, S. Pullen, T. Walter, and P. Enge, “Ionosphere Spatial Gradient Threat for LAAS: Mitigation and Tolerable Threat Space”, *Proceedings of ION 2004 Annual Meeting*, San Diego, CA., January 26-28, 2004.
- [10] M. Luo, S. Pullen, A. Ene, D. Qiu, T. Walter, and P. Enge, “Ionosphere Threat to LAAS: Updated Model, User Impact, and Mitigations,” *Proceedings of ION GNSS 2004*, Long Beach, CA., September 21-24, 2004, pp. 2771-2785.

- [11] J. Lee, M. Luo, S. Pullen, Y.S. Park, M. Brenner, and P. Enge, "Position-Domain Geometry Screening to Maximize LAAS Availability in the Presence of Ionosphere Anomalies," *Proceedings of ION GNSS 2006*, Fort Worth, TX, September 26-29 , 2006, pp. 393-408.
- [12] S. Ramakrishnan, J. Lee, S. Pullen, and P. Enge, "Targeted Ephemeris Decorrelation Parameter Inflation for Improved LAAS Availability during Severe Ionosphere Anomalies", *Proceedings of ION 2008 National Technical Meeting*, San Diego, CA, January 28-30, 2008.
- [13] *Minimum Operational Performance Standards for GPS Local Area Augmentation System Airborne Equipment*. Washington, D.C., RTCA SC-159, WG-4A, DO-253B, June 26, 2007.
- [14] Minimum Aviation System Performance Standards: Required Navigation Performance for Area Navigation. Washington, D.C., RTCA SC-181, DO-236B, October 28, 2003.